ARL-TN-0926 ● Oct 2018

US Army Research Laboratory

Investigation of Electrical Power Degradation in Beta Photovoltaic (βPV) and Beta Voltaic (βV) Power Sources Using ^{63}Ni and ^{147}Pm

by V Maren Berman, Marc Litz, Johnny Russo

NOTICES

Disclaimers

The findings in this report are not to be construed as an official Department of the Army position unless so designated by other authorized documents.

Citation of manufacturer's or trade names does not constitute an official endorsement or approval of the use thereof.

Destroy this report when it is no longer needed. Do not return it to the originator.

ARL-TN-0926 ● OCT 2018

US Army Research Laboratory

Investigation of Electrical Power Degradation in Beta Photovoltaic (βPV) and Beta Voltaic (βV) Power Sources Using ^{63}Ni and ^{147}Pm

by V Maren Berman
Sherwood High School, Olney, MD

Marc Litz and Johnny Russo
Sensors and Electron Devices Directorate, ARL

REPORT DOCUMENTATION PAGE

Form Approved
OMB No. 0704-0188

1. REPORT DATE *(DD-MM-YYYY)*	2. REPORT TYPE	3. DATES COVERED (From - To)
October 2018	Technical Note	1 June–22 August 2018

4. TITLE AND SUBTITLE
Investigation of Electrical Power Degradation in Beta Photovoltaic (βPV) and Beta Voltaic (βV) Power Sources Using ^{63}Ni and ^{147}Pm

5a. CONTRACT NUMBER

5b. GRANT NUMBER

5c. PROGRAM ELEMENT NUMBER

6. AUTHOR(S)
V Maren Berman, Marc Litz, Johnny Russo

5d. PROJECT NUMBER

5e. TASK NUMBER

5f. WORK UNIT NUMBER

7. PERFORMING ORGANIZATION NAME(S) AND ADDRESS(ES)
US Army Research Laboratory
ATTN: RDRL-SED-E
Aberdeen Proving Ground, MD 21005

8. PERFORMING ORGANIZATION REPORT NUMBER
ARL-TN-0926

9. SPONSORING/MONITORING AGENCY NAME(S) AND ADDRESS(ES)

10. SPONSOR/MONITOR'S ACRONYM(S)

11. SPONSOR/MONITOR'S REPORT NUMBER(S)

12. DISTRIBUTION/AVAILABILITY STATEMENT
Approved for public release; distribution is unlimited.

13. SUPPLEMENTARY NOTES

14. ABSTRACT
Radioisotope power sources are attractive due to their power delivery capability that spans decades and comes from the long half-lives of beta (β)-emitting isotopes. Further advantages in combat are their low mass and low volume compared with chemical power sources. Damage to wide-band-gap semiconductors has been measured for high-flux-space applications. Less effort has been put into characterizing damage from lower-flux environments. Material damage is reported for two configurations. The electrical outputs from indium gallium phosphide β-photovoltaic cells with an initial exposure of 50 mCi of ^{63}Ni nickel (99-year half-life) have been measured over a period of 19 months. The total energy conversion efficiency for this geometry is only 0.2%, and the electrical output is compared with the isotope decay over time. No measurable damage is measured within calculated statistical variation. Additionally, the electrical outputs from silicon carbide β-voltaic (βV) cells with an initial exposure of 46 mCi of ^{147}Pm promethium (2.62-year half-life) have been measured over a period of 2.3 months. Initial results show the βV cell half-life to be 0.88 year, reduced significantly from the 2.6-year half-life of ^{147}Pm alone.

15. SUBJECT TERMS
isotope power source, wideband gap damage, beta flux damage, energy conversion, silicon carbide (SiC) damage, indium gallium phosphide (InGaP) damage

16. SECURITY CLASSIFICATION OF:			17. LIMITATION OF ABSTRACT	18. NUMBER OF PAGES	19a. NAME OF RESPONSIBLE PERSON
a. REPORT	b. ABSTRACT	c. THIS PAGE			Marc Litz
Unclassified	Unclassified	Unclassified	UU	36	19b. TELEPHONE NUMBER (Include area code) 301-394-5556

Contents

List of Figures

List of Tables

1. Introduction

Radioisotope power sources are attractive due to their power delivery capability that spans decades and comes from the long half-lives of beta (β)-emitting isotopes. Further advantages in combat are their low mass and low volume compared with chemical power sources. Damage to wide-band-gap semiconductors has been measured for high-flux-space applications. Less effort has been put into characterizing damage from lower-flux environments.[1–3]

The purpose of this research is to develop an alternative to the currently used chemical power sources. The goal is for this alternative power source to have a long lifetime so that Soldiers are able to expend less capital on missions to replace power sources whose energy storage has been exhausted. Currently used chemical power sources are quickly drained of energy, heavy to carry, and space consuming. Soldiers' lives are put at risk while executing power-source replacement missions. Radioisotope power sources address this problem because they are able to last for years on end and have a relatively low mass and volume compared with chemical power sources. This report covers the evaluation of measured damage to wide-band-gap semiconductors from β-emitting isotopes, specifically the effects of nickel 63 (^{63}Ni) (99-year half-life) and promethium 147 (^{147}Pm) (2.62-year half-life) on indium gallium phosphide (InGaP) photovoltaic (PV) cells and silicon carbide (SiC), respectively. Experiment descriptions, results and conclusions, and future work are discussed along with necessary background information.

2. Experimental Configuration

β-photovoltaic (βPV) and β-voltaic (βV) devices work by harnessing the energy contained in β-emitting isotopes. βPVs go through two stages of energy conversion (Fig. 1), whereas βVs go through one stage. In βPV devices, optical energy is created from nuclear energy through β-particles interacting with zinc sulfide (ZnS). The optical energy is then converted to electrical energy in a PV cell. In the βV device, there is a direct conversion of nuclear energy to electrical energy (Fig. 2).

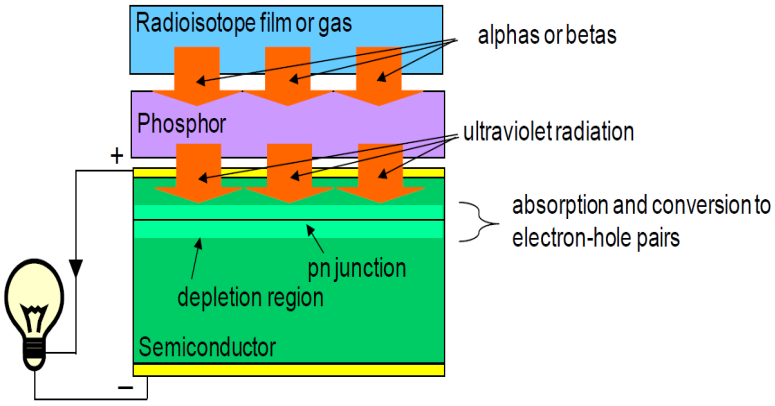

Fig. 1 Two-step process of indirect energy conversion. Radiation from decaying isotopes creates excitations in a phosphor that emits photons. The photons are collected by PV cells and converted to electrical current.[4]

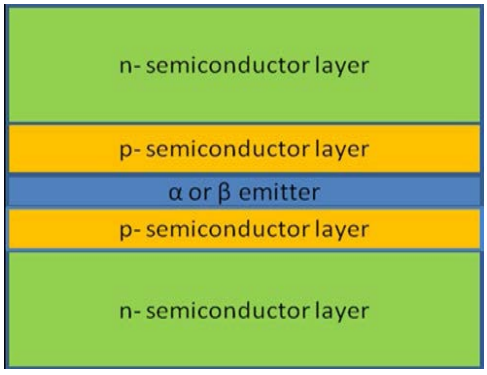

Fig. 2 The most straightforward approach is to utilize direct-energy conversion. Alphas, betas, or gammas create electron hole pairs in semiconductors. The internal electric fields of the semiconductor pull out the free-charge and current flow is generated.[4]

2.1 βPV Experiment Description

The experiment consisted of two InGaP βPV cells (1-cm^2 area), #ML1 and #ML6, which both had an initial input of 50 mCi of ^{63}Ni and an output of electrical current. The difference between the two devices is the spacing of the ^{63}Ni/phosphor film and the InGaP PV cell (Fig. 3). For this experiment, the phosphor used was ZnS. An electrical current was produced by the devices and then measured by a Keithley 485 Picoammeter. The electrical current output was then recorded in an Excel spreadsheet by a Raspberry Pi data-acquisition system. The structure of the data file is shown in Appendix A. The electrical current was recorded once every minute. Although the energy was converted twice in these βPVs, there were three opportunities for energy loss. Energy is lost when 1) it is converted from nuclear energy to optical energy through the β-particle's interactions with the phosphor,

2) photons travel through space from the ^{63}Ni/ phosphor film to the InGaP PV cell, and 3) optical energy is converted to electrical energy in the InGaP PV cell. The term "optical-space attenuation" (Table 1) refers to the energy that is lost as photons travel from the ^{63}Ni/ phosphor film to the InGaP PV cell. This value is dependent on the geometrical configuration of the device. At best, when the ^{63}Ni/phosphor film layer is thin, 50% of the photons could contribute to energy deposited in the energy converter; however, this percentage was realized when the two layers had direct contact. In Table 1, the energy percentage lost in each step is shown, along with the theoretical total energy conversion efficiency (TECE).

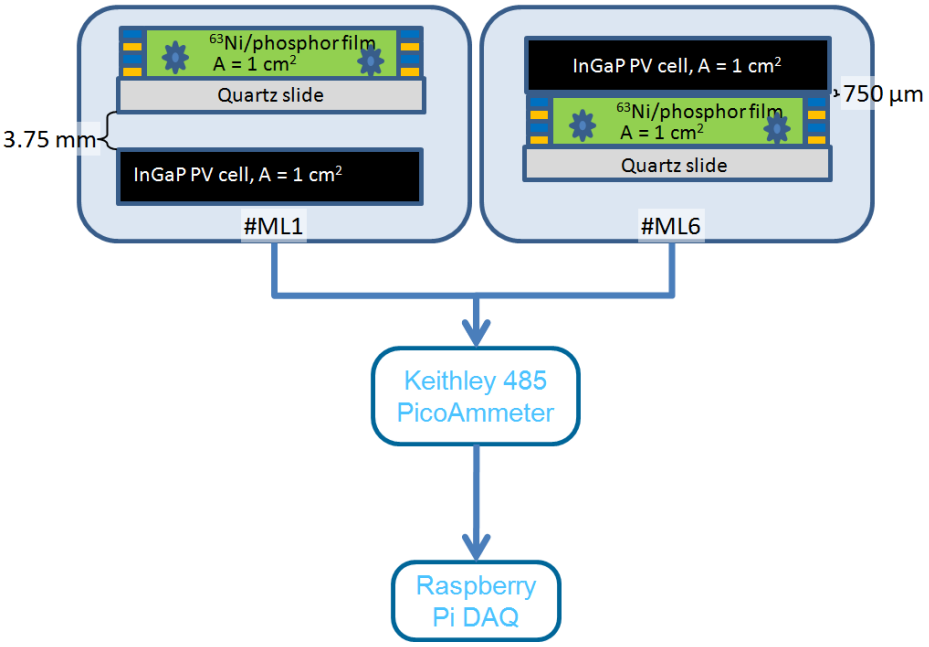

Fig. 3 Schematic of βPV experimental setup of devices #ML1 (left) and #ML6 (right)

Table 1 Energy balance for βPV devices #ML1 and #ML6

	Percent energy retained			
Device	**Nuclear-optical (%)**	**Optical-space attenuation (%)**	**PV-electrical (%)**	**Theoretical TECE (%)**
#ML1	18.9 [5]	26.09	16 [6]	0.79
#ML6		42.43		1.25

Overall, approximately 0.79% of the initial nuclear energy is expected to be converted in #ML1, and 1.25% of the initial energy is expected to be converted in #ML6. The calculations that went into the optical-space attenuation percentage are explained in Section 2.3.

2.2 βPV Experiment Results

Electrical current data were collected once every minute from two devices over a period of 19 months for a total of 1,072,057 data points. The raw data are shown in Fig. 4, and the smoothed data are shown in Fig. 5. The MatLab code that reads data and calculates power results is shown in Appendix B and Appendix C. The time increment between data points taken from the devices was 1 min.

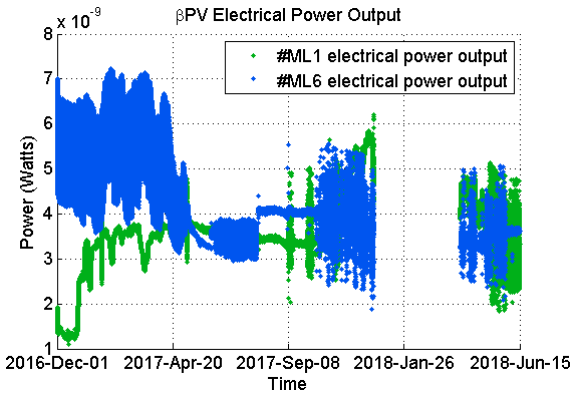

Fig. 4 Power data derived from raw electrical current data collected from devices #ML1 and #ML6 times measured voltage of βPV (0.45 V)[4]

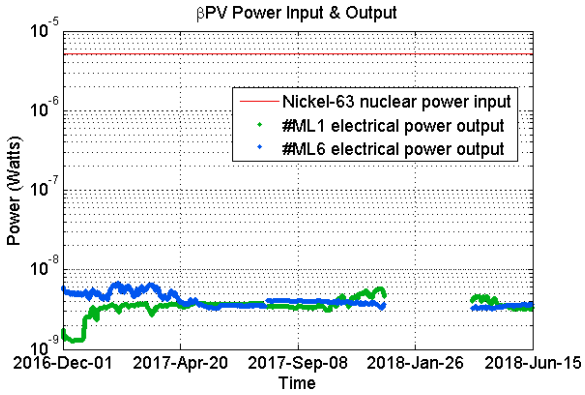

Fig. 5 Data analysis resulted in statistical means of 7.78 nW for #ML1 and 9.60 nW for #ML6. There is a difference of 3 orders of magnitude between power output of #ML1 and #ML6 and power input of ^{63}Ni.

Electromagnetic noise in the data was observed and found to be generated by other experiments and devices housed nearby in the same building on the Oak Ridge National Laboratory campus. Due to these factors, the useful results from the experiment were only in that it allowed the calculation of statistical values. The relationship between the nuclear input power (P_{nuc}) and the electrical output power (P_{elec}), shown in detail by the energy balance equations, is still of significance, regardless of noise in the data. To determine the electrical power from the raw electrical current data, each data point was multiplied by 0.45 V, the measured

voltage of the InGaP PV.[4] The equation for initial nuclear activity (power) of ^{63}Ni is

$$P_{0nuc} = (50\ \text{mCi})\ (3.7\times10^{7}\ \tfrac{\text{dec}}{\text{s}})\ (17.6\ \tfrac{\text{keV}}{\text{dec}})\ (1.6\times10^{-16}\ \tfrac{\text{J}}{\text{keV}}) = \tfrac{\text{J}}{\text{s}} = 5.2096\times10^{-6}\ \text{W}. \quad (1)$$

In Eq. 1, millicuries (mCi) are a measure of decays per second. One millicurie is equal to 3.7×10^{7} decays per second. ^{63}Ni has an average of 17.6 kilo-electron-volts (KeVs) per decay. One KeV is equal to 1.6×10^{-16} J. When these values are multiplied, the units left over are Joules per second. This is equal to watts, a unit of power. From the initial 50 mCi, the nuclear power is 5.2096×10^{-6} W.

The equation for nuclear power input as the ^{63}Ni decays is

$$P_{nuc} = (5.2096\times10^{-6})\ (e^{(-1.9169\times10^{-5})\,(t)}). \quad (2)$$

Equation 2 follows the format of radioactive decay ($N = N_0 e^{-\lambda t}$). The coefficient value in this equation is the initial nuclear power from Eq. 1. The λ (decay constant) of 1.9169×10^{-5} was found using algebra. Since the half-life is known, at t = 99 years, N = 25 mCi and N_0 = 50 mCi. Since those three variables are known, λ can be deduced. In this equation, t is in the units of days and represents the amount of time that has passed.

2.3 Optical-Space Attenuation Calculations

The optical-space attenuation values (Table 1) were calculated as follows. The subsequent calculations were done wholly in 2 dimensions (Fig. 6). The varying factors are 1) where the β-emitting isotope being considered is along the ^{63}Ni/phosphor film, E, and 2) the distance between the ^{63}Ni/phosphor film and the InGaP PV cell. From the point of the β-emitting isotope (E), two lines were drawn (CE and CD). The lines were to either end of the line segment (points C and D) representing the InGaP PV cell. The angle, α, that was formed by CED (the two line segments drawn) was measured using the law of cosines. To get the efficiency for the particular point of E, the angle measure of α was divided by 360° to determine what percentage of β-emission from E hit the segment CD. Next, the efficiency was plotted against the spacing between segments AB and CD (a range of 0–4 cm) using multiple lines to represent each point source of β-emission. The average of the percentages for 3.75- and 750-μm spacing was then taken. These averages are shown in column 3 of Table 1. Photons that were absorbed or otherwise disrupted in their path from the phosphor film to the PV cell were not accounted for.

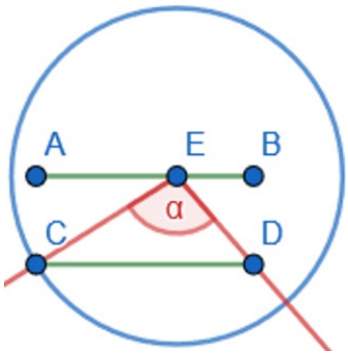

Fig. 6 Calculations to obtain optical-space attenuation value. Segment AB is ^{63}Ni/ phosphor film. Segment CD is an InGaP PV cell. Point E is the sample location of β-emitting point source. α is angle CED.

2.4 βPV Experiment Conclusion

While the data that came out of this experiment were corrupted by electrical noise, statistical metrics were calculated (Table 2). These values enabled confirmation of the energy balance within the system (Table 1). Analysis of data resulted in several useful outcomes. First, an energy balance was established for the two configurations used in #ML1 and #ML6, and second, a method was established for finding the optical-space attenuation values for similar configurations. The experimental limitations of the building that housed the experiment were also found, a significant one being that, for the relevant data to be seen through the electromagnetic noise, output current must be on the order of tens of nanoamperes (nAs) as seen in the βV experiment rather than on the order of nanoamperes as measured in the βPV experiment. Damage to the InGaP PV cell is not observed.

Table 2 Statistical metrics of oversampled βPV data compare well to the energy balance calculation (Table 1). Experimental TECE is 0.15% for #ML1 and 0.18% for #ML6.

Device	μ	σ
#ML1 electric power (nW)	7.777	1.608
#ML6 electric power (nW)	9.598	2.018

2.5 Experiment Description

Promethium chloride ($PmCl_3$) was deposited on an SiC semiconductor energy converter, 5 mm on a side (Fig. 7). A reservoir was used to contain the isotope layer and identify the activity per unit area. The electrical current was measured (using Raspberry Pi-controlled Picoammeter described in Fig. 3) after applying a liquid-form $PmCl_3$ isotope. The experimental results for two independent SiC devices (#26 and #34) are shown in Fig. 8.

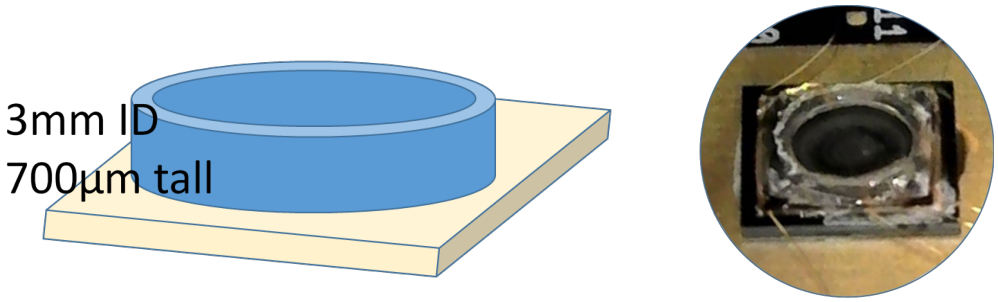

Fig. 7 (left) Reservoir mounted on SiC chip and (right) low-resolution microscope image of βV cell

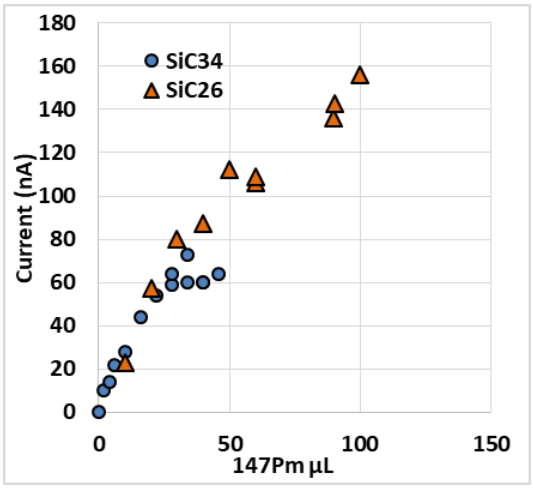

Fig. 8 Current (nanoamperes) is measured as a function of microliters of $PmCl_3$ applied to device. Absorption of moisture is visible for Device #26 at the 25-µl level. Heat was applied and electrical power output was restored.

Data were taken once every 40 min over a period of 2.3 months for a total of 2594 data points. The time increment between each data point is greater than it was for the βPV experiment because an eight-way splitter box was fabricated to use one Picoammeter. Nuclear energy is converted to electrical energy in the βV cell using SiC and gallium nitride (GaN) semiconductors. The GaN result was too low to be measurable using the Picoammeter. The nuclear power contained in the radioisotope layer was calculated from the initial activity of 46 mCi of ^{147}Pm. The equation for initial nuclear activity (power) of ^{147}Pm is

$$P_{0nuc} = (46\ \text{mCi})\ (3.7\times10^{7}\ \tfrac{\text{dec}}{\text{s}})\ (62\ \tfrac{\text{keV}}{\text{dec}})\ (1.6\times10^{-16}\ \tfrac{\text{J}}{\text{keV}}) = \tfrac{\text{J}}{\text{s}} = 1.6884\times10^{-5}\ \text{W}. \quad (3)$$

In Eq. 3, nuclear power is shown. ^{147}Pm has an average of 62 KeV per decay. When these values are multiplied, the units left are Joules per second, equal to watts. From the initial 46 mCi, the nuclear power is 1.6884×10^{-5} W.

2.6 βV Experiment Results

This experiment resulted in data (shown in Appendix D) with little noise compared with the βPV data described in Section 2.2. MatLab code was written to read the data file and calculate decay rate (shown in Appendix E). The equation of the fitted exponential curve to the βV electrical power output (Fig. 9) is

$$P_{elc}=P_0 e^{-\lambda t}=(1.387\times10^{-7})\,(e^{(-2.146\times10^{-3})\,(t)}). \quad (4)$$

Following the format of a radioactive decay equation, Eq. 4 was found using a curve fit tool provided by MatLab (cftool). The coefficient of 1.387×10^{-7} represents the initial electrical power of the βV cell. The λ of 2.146×10^{-3} represents the decay rate of the electrical power output. Time, t, is in units of days and represents the amount of time that has passed. This curve shows a half-life of 0.88 year, resulting from the natural log of 1/2 divided by λ.

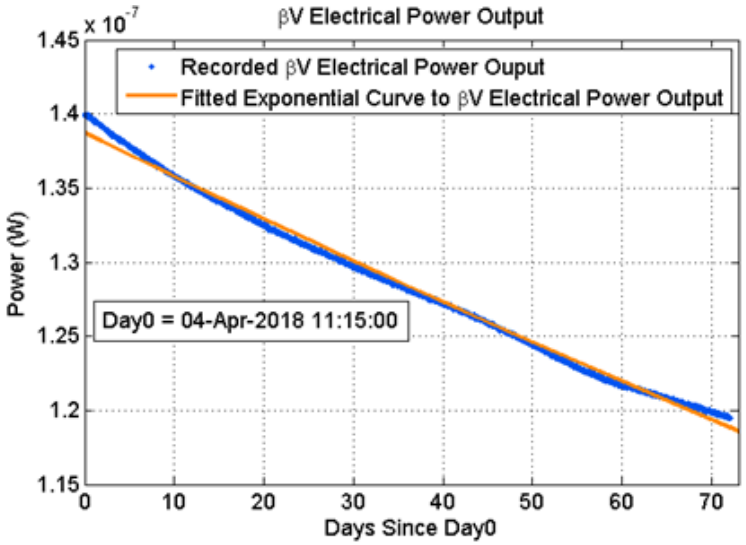

Fig. 9 Data analysis resulted in an exponential curve fitted to the βV power data

Figure 10 shows the electrical power output along with the power input. The equation for nuclear power input as the ^{147}Pm decays is

$$P_{nuc}=(1.6884\times10^{-5})\,(e^{(-7.2433\times10^{-4})\,(t)}). \quad (5)$$

Equation 5 follows the format of radioactive decay. The coefficient value in this equation is the initial nuclear power found in Eq. 3. The λ of 7.2433×10^{-4} was calculated from the half-life of τ = 2.62 years, N = 46 mCi, and N_0 = 23 mCi. $N=N_0e^{-\lambda t}$. Since three variables are known, λ (decay constant) can be deduced. In this equation, t is in units of days and represents the amount of time that has passed.

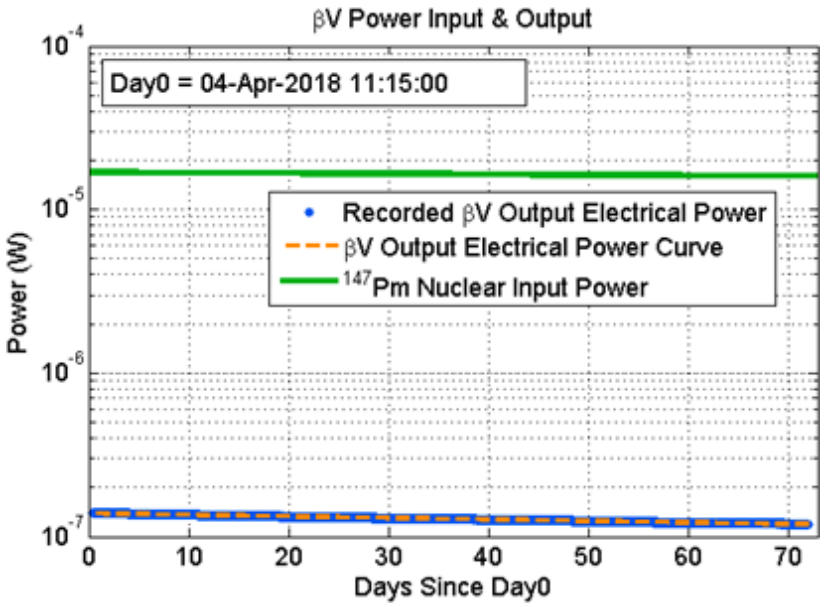

Fig. 10 βV power data derived from raw electrical current data times measured voltage of βV (2.2 V)[7]

Since the electrical power output declines more rapidly than the nuclear power input, there must be another factor affecting the net electrical output. There are two factors to consider: 1) the degradation of the SiC material subjected to radiation exposure,[8] which would change the energy conversion efficiency of the SiC, η_{SiC}, and 2) the reduction in effective surface activity on the SiC, η_{src}, which can be affected by moisture absorption. These factors are expressed in Eq. 3. The power source half-life as calculated from raw electrical output would result in 0.88 year. However, it was measured during the experimental application of liquid-form isotope that the effective surface activity was reduced by 20% within 24 h because of absorption of moisture by the $PmCl_3$ at standard temperature and pressure. The effective surface activity is a measure of the amount of isotope activity that exits the isotope layer and reaches the energy converter after self-attenuation of the isotope medium. A reduced surface activity effect was confirmed during the isotope loading/deposition by heating the device and observing that the electrical current increase by 25% as a result of the heating. This effect can be observed in the data from Device #34 shown in Fig. 11 at the 34-mCi level. During that activity deposition level we stopped adding more isotope, waited overnight, and heated/removed moisture from the sample.

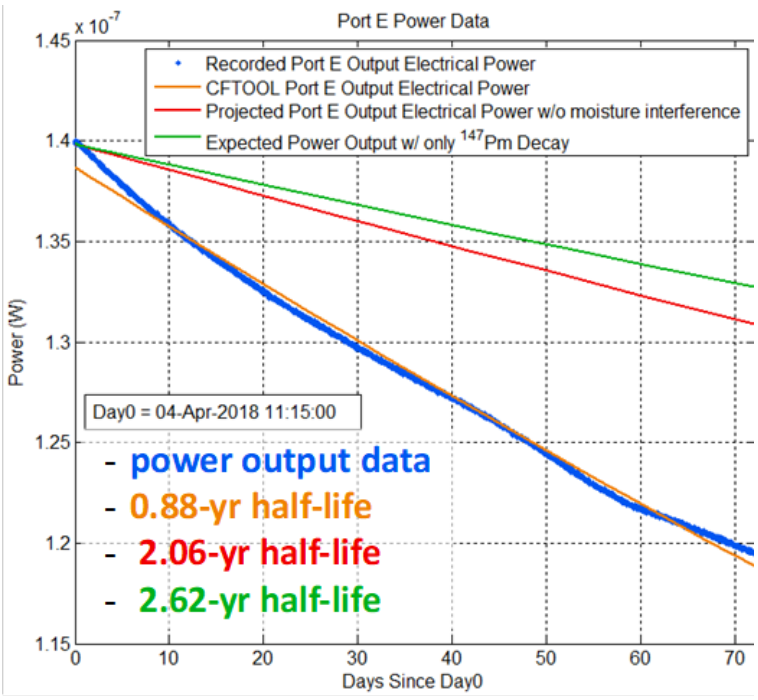

Fig. 11 Electrical power output data and nuclear power input reference lines. Also shown is the first attempt at quantifying moisture effect on power output in red.

The increase of 25% effective surface activity after heating (moisture evaporation) allows a better understanding of the parameters affecting the experiment. If the moisture content decreased the electrical output by 25% in the experiment on Device #34, then the source efficiency, η_{src}, can be recalculated from Eq. 3 to make up for this loss to get a better understanding of efficiencies. Both η_{src} and η_{SiC} contribute to net electrical power reduction. (For the estimate that follows, it is assumed that the energy converter device efficiency of 16% remains constant.)[9] The power source half-life as calculated from raw electrical output data would be 0.88 year instead of the moisture modified result of 2.06 years. The results of system decay calculations that prioritize moisture absorption over SiC damage are shown in Fig. 11. The curve in Fig. 12 shows η_{src} from the measurement data compared with numerical calculations from MCNPX code.[10] Both curves show a similar trend with increasing applied activity. The MCNPX numerical values shown in Fig. 12 result from varying the layer thickness (and therefore activity) applied to the surface of an SiC device. By comparing the numerically calculated source efficiency and the measured source efficiency, the moisture effects can begin to be understood and calculated. The numerical calculation assumed a $PmCl_3$ density of 1.5 g/cc, but it appears that a lower density of approximately 1.1 g/cc would provide a better match to the measured data.

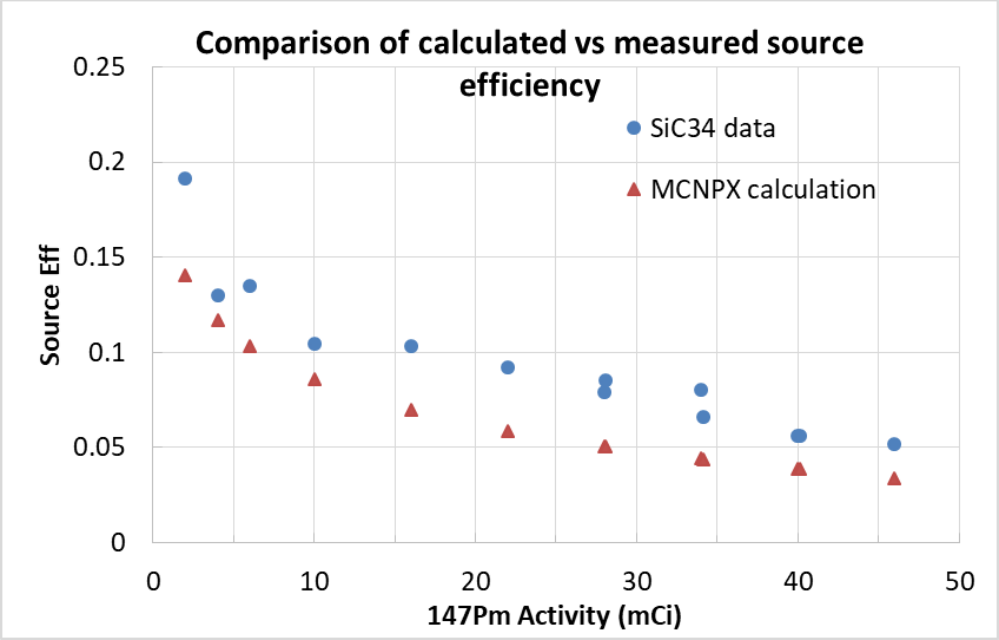

Fig. 12 Numerically calculated source efficiency and measured source efficiency. Measured results assume only 16% uniform SiC efficiency[8] with no modification for known moisture absorption.

2.7 βV Experiment Conclusion

Reduction in electrical power output beyond the decay of the isotope was measured. Two factors contributed to the reduction in electrical power. The first was damage to the SiC in the βV cell using ^{147}Pm. The damage changes the energy conversion efficiency of the SiC, η_{SiC} in Eq. 3. The second factor was the reduction in effective surface activity of the isotope layer on the SiC energy converter because of increasing moisture content in the unsealed experimental laboratory setting: a worst-case calculation of 5% for η_{src} results if a constant 16% η_{SiC} is assumed. A half-life of approximately 2.06 years, reduced from 2.62 years for isotope half-life is a more realistic result when including the absorbed moisture content in $PmCl_3$. As more data are acquired in this long-term measurement, it is expected that the moisture absorption contributing to η_{src} could be better deconvoluted, and any damage to SiC (change in η_{SiC} over time) from $PmCl_3$ will be identified.

Clarification of the level of moisture content absorbed in the liquid-form isotope layers must be identified before quantitative rates of decay to energy converter can be identified.

3. Conclusion

No change in efficiency of InGaP was measured when subjected to ^{63}Ni in the βPV experiment. The TECE of the βV power source ranges from 0.83% at the start to 0.74% after 2.3 months, an eight times greater TECE than that of either βPV device #ML1 or #ML6. The higher η of the βV system is primarily attributed to the reduction in losses from a one-step (direct energy conversion) to a two-step (indirect energy conversion) path toward electrical current.

SiC exposed to ^{147}Pm in the βV experiment showed change in net electrical output beyond isotope decay. The effective half-life of ^{147}Pm on SiC raw data was calculated to be 0.88 year because of two factors: the moisture absorption in the isotope layer, ηsrc, and the damage from ^{147}Pm beta emission on the SiC, ηSiC. These two factors cannot be completely deconflicted at this time. However, an explanation (moisture absorption) resulting in a calculated half-life of 2.06 years has been described. Long-term data continue to be measured. Experiments are planned to confirm the level of moisture content to better define any damage that may be present in the SiC because of the 24-keV end-point energy of the $PmCl_3$ emission. The results presented represent only a first look.

Since the longevity of the devices was a main goal in driving this experiment, more research will have to be performed to understand the moisture effects, which can be avoided with an epoxy sealant.

The ^{63}Ni-loaded βPV power sources have a 99-year lifetime, and the ^{147}Pm-loaded SiC βV power sources have an effective half-life of 2.06 years, reduced from 2.62 years. The differences between the βPV and βV experiments that made the latter results more useful are the tens of nanoamperes of signal strength required to overcome the noise in the radiation facility compared with the hundreds of picoamperes of current output from the former.

4. Future Work

To continue this process of improving upon radioisotope and isotope power sources, further measurements will be conducted on increasing both source efficiency and device efficiency to add to power system longevity. The βPV experiment will be repeated with higher activity levels to produce 100 nA of measurable electrical current. The required activity for radioisotopes of interest combined with energy converter is shown in Table 3. The activity shown in column 1 of Table 3 is the minimum amount of ^{147}Pm activity required to produce a 100-nA level of measureable current for SiC (column 7) and GaN (column 8). In addition, experimental procedures reducing the 25-ft cables used in this experiment

to 6-ft electromagnetically shielded cables are in progress. For completeness and improved accuracy, the optical-space attenuation values will be calculated in a 3-D space.

Table 3 Activity required to achieve a 10-nA measurable electrical signal from SiC and GaN energy converters is tabulated

				ECE 0.12	ECE 0.05	V 2.2	V 1.5
				SiC	GaN	SiC	GaN
mCi	keV/decay	P_{nuc} (W)	Source efficiency	P_{elec} (W)		I_{out} (A)	
0.08	5000	2.368E-06	0.16	4.55E-08	1.89E-08	2.07E-08	1.26E-08
0.8	62	2.936E-07	0.14	4.93E-09	2.06E-09	2.24E-09	1.37E-09
20	17	2.013E-06	0.015	3.62E-08	1.51E-08	1.65E-08	1.01E-08
100	6	3.552E-06	0.1	4.26E-08	1.78E-08	1.94E-08	1.18E-08

The η_{SiC} will be measured independently using a 100-mCi foil calibration source to identify any change over time. The η_{src} will be evaluated separately using epoxy sealants to minimize or avoid any change in η_{SiC} because of moisture absorption.

5. References

1. Summers G, Burke E, Shapiro P, Messenger S, Walters R. Damage correlations in semiconductors exposed to gamma, electron and proton radiations. IEEE Transactions on Nuclear Science. 1993;40(6):1372–1379.

2. Langley J, Litz M, Russo J, William R Jr. Design of alpha voltaic power source using americium 241 (^{241}Am) and diamond with a power density of 10 mW/cm^3. Aberdeen Proving Ground (MD): Army Research Laboratory (US); 2017 Oct. Report No.: ARL-TR-8189.

3. Rybicki G, Vargas-Aburto C, Uribe R. Silicon carbide alphavoltaic battery. Proceedings of the 25th IEEE Photovoltaic Specialists Conference; 1996.

4. Litz M. Isotope beta-battery approaches for long-lived sensors. Aberdeen Proving Ground (MD): Army Research Laboratory (US); 2014 Aug. Report No.: ARL-TR-7048.

5. Russo J, Litz M, Ray W, Smith B, Moyers R. A radioluminescent nuclear battery using volumetric configuration: ^{63}Ni solution/ZnS:Cu, Al/InGaP. Applied Radiation and Isotopes. 2017;130:66–74.

6. Russo J, Litz M, Ray W. Low light illumination study on commercially available homojunction photovoltaic cells. Applied Energy. 2017;191:10–21.

7. Litz M, Blaine K. Isotope generated electron density in silicon carbide direct energy converters. Aberdeen Proving Ground (MD): Army Research Laboratory (US); 2006 Oct. Report No.: ARL-TR-3964.

8. Olsen LC. Review of betavoltaic energy conversion. Proceedings of the 12th Space Photovoltaic Research and Technology Conference; 1993 May 1; Washington, DC. p. 256–267.

9. Thomas C, Portnoff S, Spencer MG. High efficiency 4H-SiC betavoltaic power sources using tritium radioisotopes. Applied Physics Letters. 2016;108(1).

10. Pelowitz DB. MCNPX user's manual. Version 2.7.0. Los Alamos (NM): Los Alamos National Laboratory; 2011 Apr. Publication No.: LA-CP-11-00438.

Appendix A. β-Photovoltaic (βPV) Data Files

The following data file shown is an example of the layout that was read in the β-photovoltaic (βPV) data analysis. Files read to create graph figures for βPV were *FINAL_ML1_fulldata_compilation.csv* and *INAL_ML6_fulldata_compilation.csv*. This file was read-in using the program exhibited in Appendixes B and C. It was read into seven different matrices, one each for the year, month, day, hour, minute, second, and electrical current. The data file that was read-in is a compilation of the multiple data files created by the βPV experiment process. The compilation file removed an unnecessary blank column that was included in the hourly data files.

2017-08-04,02:00:0,7.731360E-09
2017-08-04,02:02:0,7.740752E-09
2017-08-04,02:04:0,7.744843E-09
2017-08-04,02:06:0,7.721949E-09
2017-08-04,02:08:0,7.740753E-09
2017-08-04,02:10:0,7.759548E-09
2017-08-04,02:12:0,7.768952E-09
2017-08-04,02:14:0,7.750155E-09
2017-08-04,02:16:0,7.734128E-09
2017-08-04,02:18:0,7.778340E-09
2017-08-04,02:20:0,7.713496E-09
2017-08-04,02:22:0,7.750031E-09
2017-08-04,02:24:0,7.739047E-09
2017-08-04,02:26:0,7.744059E-09
2017-08-04,02:28:0,7.734887E-09
2017-08-04,02:30:0,7.721962E-09
2017-08-04,02:32:0,7.736444E-09
2017-08-04,02:34:0,7.790471E-09
2017-08-04,02:36:0,7.745976E-09
2017-08-04,02:38:0,7.750156E-09
2017-08-04,02:40:0,7.750147E-09
2017-08-04,02:42:0,7.750152E-09
2017-08-04,02:44:0,7.750149E-09
2017-08-04,02:46:0,7.744371E-09
2017-08-04,02:48:0,7.767527E-09
2017-08-04,02:50:0,7.763844E-09
2017-08-04,02:52:0,7.782499E-09
2017-08-04,02:54:0,7.761861E-09
2017-08-04,02:56:0,7.721960E-09
2017-08-04,02:58:0,7.740754E-09
2017-08-02,14:48:30,7.086905E-09
2017-08-02,14:50:0,7.090653E-09
2017-08-02,14:52:0,7.089219E-09
2017-08-02,14:54:0,7.149943E-09
2017-08-02,14:56:0,7.094602E-09
2017-08-02,14:58:0,7.107003E-09
2017-08-02,15:00:0,7.086023E-09
2017-08-02,15:02:0,7.094961E-09
2017-08-02,15:04:0,7.140935E-09
2017-08-02,15:06:0,7.442072E-09
2017-08-02,15:08:0,7.450395E-09
2017-08-02,15:10:0,7.453710E-09
2017-08-02,15:12:0,7.462122E-09
2017-08-02,15:14:0,7.482338E-09
2017-08-02,15:16:0,7.494624E-09
2017-08-02,15:18:0,7.477599E-09
2017-08-02,15:20:0,7.495512E-09
2017-08-02,15:22:0,7.488762E-09
2017-08-02,15:24:0,7.499817E-09
2017-08-02,15:26:0,7.486992E-09
2017-08-02,15:28:0,7.506496E-09
2017-08-02,15:30:0,7.477602E-09
2017-08-02,15:32:0,7.489582E-09
2017-08-02,15:34:0,7.521654E-09
2017-08-02,15:36:0,7.478760E-09
2017-08-02,15:38:0,7.476098E-09
2017-08-02,15:40:0,7.499859E-09

Appendix B. β-Photovoltaic (βPV) Data Files MatLab Read Routine A

The following read routine was used to create Fig. 4 in the report. It is called *newplotml1ml6.m* and reads the files discussed in Appendix A. The figure it creates shows every data point of devices #ML1 and #ML6.

```
close all;clear all;
% Plot ML1, Ml6, (Electrical Power) and Nuclear Power
% read in ML1 data
fileID=fopen('FINAL_ML1_fulldata_compilation.csv');

data1=textscan(fileID,'%f %*1c %f %*1c %f %*1c %f %*1c %f %*1c %f %*1c %f %*1c %f');

year1=data1{1,1};
mo1=data1{1,2};
dy1=data1{1,3};
hr1=data1{1,4};
mi1=data1{1,5};
se1=data1{1,6};
Amp1=data1{1,7};
serialdate1=datenum(year1,mo1,dy1,hr1,mi1,se1);

% read in ML6 data
fileID=fopen('FINAL_ML6_fulldata_compilation.csv');

data6=textscan(fileID,'%f %*1c %f %*1c %f %*1c %f %*1c %f %*1c %f %*1c %f %*1c %f');

year6=data6{1,1};
mo6=data6{1,2};
dy6=data6{1,3};
hr6=data6{1,4};
mi6=data6{1,5};
se6=data6{1,6};
Amp6=data6{1,7};
serialdate6=datenum(year6,mo6,dy6,hr6,mi6,se6);

%paste below section into command window
%   X ticks:
NumTicks=9;
L=get(gca,'XLim');
set(gca,'XTick',linspace(L(1),L(2),NumTicks));
datetick('x','yyyy-mmm-dd, HH:MM','keepticks','keeplimits')
%   Y ticks:
NumTicks=21;
L=get(gca,'YLim');
set(gca,'YTick',linspace(L(1),L(2),NumTicks));


red=[0.941176470588235 0 0];
orange=[0.941176470588235 0.584313725490196 0];
yellow=[0.803921568627451 0.964705882352941 0];
green=[0 0.690196078431373 0.098039215686275];
blue=[0 0.337254901960784 0.941176470588235];
purple=[0.509803921568627 0 0.823529411764706];
pink=[0.941176470588235 0 0.917647058823529];
teal=[0 0.815686274509804 0.737254901960784];

% convert mCi to nuclear power
figure(1)
    n=1;
    serialdate1n=serialdate1(1:n:end);
    serialdate6n=serialdate6(1:n:end);
    Amp1n=Amp1(1:n:end);
    Amp6n=Amp6(1:n:end);

    title('ML1 and ML6 Power Output'),ylabel('Power (Watts)'),xlabel('Time'),
    grid on,

    % Calculate Electrical power output for ML1 and ML6
    V=0.45;
    Pelc1=V.*Amp1n;
    Pelc6=V.*Amp6n;

    %plot ML1 and ML6 electrical power
    hold on
    plot(serialdate1n,Pelc1,'.','Color',green)
    hold on
    plot(serialdate6n,Pelc6,'.','Color',blue)
    grid on;
    xlim([min(serialdate1n) max(serialdate1n)])
%   X ticks:
    NumTicks=9;
    L=get(gca,'XLim');
    set(gca,'XTick',linspace(L(1),L(2),NumTicks));
    datetick('x','yyyy-mmm-dd, HH:MM','keepticks','keeplimits')
    %   Y ticks:
    NumTicks=21;
    L=get(gca,'YLim');
    set(gca,'YTick',linspace(L(1),L(2),NumTicks));
    legend('ML1 electrical power output','ML6 electrical power output')
```

Appendix C. β-Photovoltaic (βPV) Data Files MatLab Read Routine B

The following read routine was used to create Fig. 5 in the report. It is called *electricalnucml1ml6.m* and reads the files discussed in Appendix A. The figure it creates shows every data point of devices #ML1 and #ML6, along with the nuclear power.

```
close all;clear all;
% Plot ML1, Ml6, (Electrical Power) and Nuclear Power
% read in ML1 data
fileID=fopen('FINAL_ML1_fulldata_compilation.csv');

data1=textscan(fileID,'%f %*1c %f %*1c %f %*1c %f %*1c %f %*1c %f %*1c %f');

year1=data1{1,1};
mo1=data1{1,2};
dy1=data1{1,3};
hr1=data1{1,4};
mi1=data1{1,5};
se1=data1{1,6};
Amp1=data1{1,7};
serialdate1=datenum(year1,mo1,dy1,hr1,mi1,se1);

% read in ML6 data
fileID=fopen('FINAL_ML6_fulldata_compilation.csv');

data6=textscan(fileID,'%f %*1c %f %*1c %f %*1c %f %*1c %f %*1c %f %*1c %f');

year6=data6{1,1};
mo6=data6{1,2};
dy6=data6{1,3};
hr6=data6{1,4};
mi6=data6{1,5};
se6=data6{1,6};
Amp6=data6{1,7};
serialdate6=datenum(year6,mo6,dy6,hr6,mi6,se6);

red=[0.941176470588235 0 0];
orange=[0.941176470588235 0.584313725490196 0];
yellow=[0.803921568627451 0.964705882352941 0];
green=[0 0.690196078431373 0.098039215686275];
blue=[0 0.337254901960784 0.941176470588235];
purple=[0.509803921568627 0 0.823529411764706];
pink=[0.941176470588235 0 0.917647058823529];
teal=[0 0.815686274509804 0.737254901960784];

%paste below section into command window
%   X ticks:
NumTicks=9;
L=get(gca,'XLim');
set(gca,'XTick',linspace(L(1),L(2),NumTicks));
datetick('x','yyyy-mmm-dd, HH:MM','keepticks','keeplimits')
%   Y ticks:
NumTicks=21;
L=get(gca,'YLim');
set(gca,'YTick',linspace(L(1),L(2),NumTicks));

% mCi left for 63Ni
% figure(1),
a=min(serialdate1);b=min(serialdate6);c=[a b];
minute0=min(c);
a=max(serialdate1);b=max(serialdate6);c=[a b];
minutef=max(c);
e=2.71828182845905;
% mci=(50*(e^((-1.33118234700789E-08)*((x-minute0)*1440))))
% N=@(x)(50*(e^((-1.33118234700789E-08)*((x-minute0)*1440))));
% fplot(N,[minute0 minutef])
% title('Nickel-63 Decay'),ylabel('mCi of Nickel-63'),xlabel('Time'),
% grid on,

% convert mCi to nuclear power
figure(1)
    n=10;
    serialdate1n=serialdate1(1:n:end);
    serialdate6n=serialdate6(1:n:end);
    Amp1n=Amp1(1:n:end);
    Amp6n=Amp6(1:n:end);
    ml1nsmooth=smooth(serialdate1n,Amp1n,99);
    ml6nsmooth=smooth(serialdate6n,Amp6n,99);

    % mCi*3.7E7*17.6*1.6E-16=Joules(nuclear power)
    % nucP=((50*(e^((-1.33118234700789E-08)*((x-minute0)*1440))))*(3.7E7)*(17.6)*(1.6E-16))
    nucP=@(x)((50*(e^((-1.33118234700789E-08)*((x-minute0)*1440))))*(3.7E7)*(17.6)*(1.6E-16));
    fplot(nucP,[minute0 minutef],'-b')
    a=findobj('Color',[0 0 1]);
    set(a,'Color',red);
    title('Nickel-63 Power Input & Output'),ylabel('Power (Watts)'),xlabel('Time'),
    grid on,

    % Calculate Electrical power output for ML1 and ML6
    V=0.45;
    Pelc1=V.*ml1nsmooth;
    Pelc6=V.*ml6nsmooth;

    %plot ML1 and ML6 electrical power
    hold on
    plot(serialdate1n,Pelc1,'.','Color',green)
    hold on
    plot(serialdate6n,Pelc6,'.','Color',blue)

    legend('Nickel-63 nuclear power input','#ML1 electrical power output','#ML6 electrical power output')
```

Appendix D. β-Voltaic (βV) Data Files

The following data file is an example of the layout that was read-in the β-voltaic (βV) data analysis. The file read to create graph figures for βV is called *portEcompilation.csv*. This file was read-in using the program exhibited in Appendix E. It was read into seven different matrices, one each for the year, month, day, hour, minute, second, and electrical current. The data file that was read-in is a compilation of the multiple data files that were created by the βV experiment process for Port E. The compilation file removed an unnecessary blank column that was included in the original data files.

```
E,2018-04-04,11:15:0,6.355688E-08
E,2018-04-04,11:55:0,6.360835E-08
E,2018-04-04,12:35:0,6.358047E-08
E,2018-04-04,13:15:0,6.364042E-08
E,2018-04-04,13:55:0,6.360467E-08
E,2018-04-04,14:35:0,6.358200E-08
E,2018-04-04,15:15:0,6.356333E-08
E,2018-04-04,15:55:0,6.357546E-08
E,2018-04-04,16:35:0,6.358537E-08
E,2018-04-04,17:15:0,6.361881E-08
E,2018-04-04,17:55:0,6.357936E-08
E,2018-04-04,18:35:0,6.359104E-08
E,2018-04-04,19:15:0,6.357937E-08
E,2018-04-04,19:55:0,6.357315E-08
E,2018-04-04,20:35:0,6.356278E-08
E,2018-04-04,21:15:0,6.352719E-08
E,2018-04-04,21:55:0,6.359017E-08
E,2018-04-04,22:35:0,6.355803E-08
E,2018-04-04,23:15:0,6.352818E-08
E,2018-04-04,23:55:0,6.354581E-08
E,2018-04-05,00:35:0,6.352538E-08
E,2018-04-05,01:15:0,6.354750E-08
E,2018-04-05,01:55:0,6.351844E-08
E,2018-04-05,02:35:0,6.352257E-08
E,2018-04-05,03:15:0,6.353385E-08
E,2018-04-05,03:55:0,6.354146E-08
E,2018-04-05,04:35:0,6.348355E-08
E,2018-04-05,05:15:0,6.348658E-08
E,2018-04-05,05:55:0,6.349907E-08
E,2018-04-05,06:35:0,6.347667E-08
E,2018-04-05,07:15:0,6.347013E-08
E,2018-04-05,07:55:0,6.346053E-08
E,2018-04-05,08:35:0,6.346126E-08
E,2018-04-05,09:15:0,6.346886E-08
E,2018-04-05,09:55:0,6.344238E-08
E,2018-04-05,10:35:0,6.343929E-08
E,2018-04-05,11:15:0,6.346670E-08
E,2018-04-05,11:55:0,6.341475E-08
E,2018-04-05,12:35:0,6.342627E-08
E,2018-04-05,13:15:0,6.339183E-08
E,2018-04-05,13:55:0,6.339786E-08
E,2018-04-05,14:35:0,6.341671E-08
E,2018-04-05,15:15:0,6.344527E-08
E,2018-04-05,15:55:0,6.338754E-08
E,2018-04-05,16:35:0,6.341741E-08
E,2018-04-05,17:15:0,6.339245E-08
E,2018-04-05,17:55:0,6.339062E-08
E,2018-04-05,18:35:0,6.341120E-08
E,2018-04-05,19:15:0,6.336826E-08
E,2018-04-05,19:55:0,6.339192E-08
E,2018-04-05,20:35:0,6.336755E-08
E,2018-04-05,21:15:0,6.333952E-08
E,2018-04-05,21:55:0,6.335979E-08
E,2018-04-05,22:35:0,6.336943E-08
E,2018-04-05,23:15:0,6.334216E-08
E,2018-04-05,23:55:0,6.333084E-08
E,2018-04-06,00:35:0,6.335669E-08
```

Appendix E. β–Voltaic (βV) Data Files MatLab Read Routine

The read routine on the left was used to create Figs. 8 and 9 in the report. It is called *Expfitofport.m* and reads the files discussed in Appendix D. It creates four figures, only two of which are displayed in this report. The first one displayed shows the electrical power output of the βV and a line fitted to it. The second one displayed shows the same two plots along with the nuclear power input.

```
close all;clear all;

fileID=fopen('portEcompilation.csv');
data=textscan(fileID,'%*2c %f %*1c %f %*1c %f %*1c %f %*1c %f %*1c %f %*1c %f');

year=data{1,1};
mo=data{1,2};
dy=data{1,3};
hr=data{1,4};
mi=data{1,5};
se=data{1,6};
Amp=data{1,7};
serialdate=datenum(year,mo,dy,hr,mi,se);

date1=min(serialdate);
date2=max(serialdate);
e=2.71828182845905...
    ; % define e
days=(serialdate-date1)...
    ; % set each point as days since the first
dayO=min(days)...
    ; % set initial day as the first
lambda=(-log(0.5))/(365.25*2.62)...
    ; %define lambda
ElcCur=@(x)(6.360188333333333E-008).*(e.^(-lambda.*(x-dayO)))...
    ; % function for projected electrical current
ElcPwr=@(x)((1.399241433333333E-07).*(e.^(-lambda.*(x-dayO))))...
    ; % function for projected electrical power
ElcCurArray=ElcCur(days)...
    ; % array of projected electrical current for each time data was taken
EPwr=Amp.*2.2...
    ; % array of power given by device
ElcPwrArray=ElcCurArray.*2.2...
    ; % array of projected electrical power
nucP=@(x)(46.*(e.^((-lambda).*(x-dayO)))).*(3.7E7).*(62).*(1.6E-16)))...
    ; % function for Pm-147 decay POWER
NucArray=nucP(days)...
    ; % array of nuclear power for each time data was taken
EffectivePelc=@(x)(1.387e-007.*(e.^(-0.002146*(x-dayO))))...
    ; % cftool fit
EffectivePelcArray=EffectivePelc(days)...
    ; % array of electrical power for each time data was taken
ProjectedEfficiency=((EffectivePelcArray./NucArray).*100)...
    ; % array of efficiency for each time data was taken
otherdays=(0:.3:1E4);
Eff=((EPwr./NucArray).*100)...
    ; % array of actual efficiency of system
Eff2=@(x)((8.21495583942989E-3).*(e.^((-1.83142930893931E-3).*(x-dayO)))*100)...
    ; % efficiency function from dividing the two power equations
Eff2array=Eff2(days)...
    ; % array of Eff2 values for each time data was taken
modnuc=nucP(days)-(1.6744E-05)...
    ; % modified nuclear input power to compare directly with output power
PEout=@(x)((1.39825136e-007).*(e.^((-7.24325783929178E-04).*(x-dayO))))...
    ; % expected power output with 147Pm decay but not with SiC damage
Effeqn=@(x)((8.215E-3.*(e.^(-1.422E-3*(x-dayO))))*100)...
    ; % efficiency equation

% line colors
red=[0.941176470588235 0 0];
orange=[0.941176470588235 0.584313725490196 0];
yellow=[0.803921568627451 0.964705882352941 0];
green=[0 0.690196078431373 0.098039215686275];
blue=[0 0.337254901960784 0.941176470588235];
purple=[0.509803921568627 0 0.823529411764706];
pink=[0.941176470588235 0 0.917647058823529];
teal=[0 0.815686274509804 0.737254901960784];

figure(1)
plot(days,Amp,'.',days,ElcCurArray,'--r'),grid on
title('Port E Current Data'),xlabel('Days Since DayO'),ylabel('Current (A)')
legend('Recorded Port E Output Electrical Current','Projected Port E Output Electrical
Current')
annotation(figure(1),'textbox',[0.1411 0.3774 0.3205 0.06813],...
    'String',{'DayO = 04-Apr-2018 11:15:00'},...
    'BackgroundColor',[1 1 1]);

figure(2)
plot(days,EPwr,'.g'),grid on
hold on;
fplot(EffectivePelc,[dayO (365.25*2.62)],'b')
a=findobj('Color',[0 0 1]);
set(a,'Color',blue);
% hold on;
% fplot(ElcPwr,[dayO (365.25*2.62)],'--r')
% hold on;
% fplot(PEout,[0 365.25*2.62],'-.b');
% a=findobj('Color',[0 0 1]);
% set(a,'Color',purple);
xlim([0 73])
title('Port E Power Data'),xlabel('Days Since DayO'),ylabel('POwer (W)')
legend('Recorded Port E Output Electrical Power','CFTOOL Port E Output Electrical
Power',...
    'Projected Port E Output Electrical Power','Expected Power Output w/ 147Pm Decay')
annotation(figure(2),'textbox',[0.1411 0.4177 0.1456 0.02778],...
    'String',{'DayO = 04-Apr-2018 11:15:00'},...
    'BackgroundColor',[1 1 1]);

figure(3)
plot(days,EPwr,'.b',days,EffectivePelcArray,'--r'),grid on;
a=findobj('Color',[0 0 1]);
set(a,'Color',blue);
hold on;
fplot(nucP,[0 365.25*2.62],'-b');
a=findobj('Color',[0 0 1]);
set(a,'Color',green);
title('Port E Power Data'),xlabel('Days Since DayO'),ylabel('Power (W)')
legend('Recorded Port E Output Electrical Power','Port E Output Electrical Power
Curve',...
    'Pm-147 Nuclear Power')
annotation(figure(3),'textbox',[0.2078 0.5078 0.1469 0.03337],...
    'String',{'DayO = 04-Apr-2018 11:15:00'},...
    'BackgroundColor',[1 1 1]);

figure(4)
plot(days,Eff,'.','Color',blue),grid on
% hold on;
% plot(days,ProjectedEfficiency,'--','Color',red,'LineWidth',2),grid on
hold on;
fplot(Effeqn,[0 365.25*2.62],'-b');
a=findobj('Color',[0 0 1]);
set(a,'Color',red);
% hold on;
% plot(days,Eff2array,'--','Color',green,'LineWidth',2)
title('Port E Efficiency'),xlabel('Days since DayO'),ylabel('Efficiency (%)'),
legend('Actual Efficiency of System', 'Fitted Efficiency of System')
annotation(figure(4),'textbox',[0.2078 0.5078 0.1469 0.03337],...
    'String',{'DayO = 04-Apr-2018 11:15:00'},...
    'BackgroundColor',[1 1 1]);
```

List of Symbols, Abbreviations, and Acronyms

λ	decay constant
β	beta
^{63}Ni	nickel 63
^{147}Pm	promethium 147
3-D	3-dimensional
βPV	β-photovoltaic
βV	β-voltaic
GaN	gallium nitride
InGaP	indium gallium phosphide
KeV	kilo-electron-volt
mCi	millicurie
nA	nanoampere
Ni	nickel
pA	picoampere
Pm	promethium
$PmCl_3$	promethium chloride
PV	photovoltaic
SiC	silicon carbide
t	time
TECE	total energy conversion efficiency
Zn	zinc sulfide

1 (PDF)	DEFENSE TECHNICAL INFORMATION CTR DTIC OCA
2 (PDF)	DIR ARL IMAL HRA RECORDS MGMT RDRL DCL TECH LIB
1 (PDF)	GOVT PRINTG OFC A MALHOTRA
2 (PDF)	ARL RDRL SED E M LITZ J RUSSO